AIAA 2003-0399

Development of Laser-Induced Thermal Acoustic (LITA) Measurements for Gas Turbine Flows

T. Rossmann, K.C. Moore, and T.H. Sobota
Advanced Projects Research, Inc.
La Verne, CA

41st Aerospace Sciences Meeting & Exhibit
6–9 January 2003
Reno, Nevada

DEVELOPMENT OF LASER-INDUCED THERMAL ACOUSTICS (LITA) MEASUREMENTS FOR GAS TURBINE FLOWS

Rossmann, T.*, Moore, K.C.†, and Sobota, T.H.‡
Advanced Projects Research, Inc.
La Verne, CA 91750

Transient grating spectroscopy and its ability to make accurate measurements of thermodynamic quantities at high density conditions make them attractive for optical measurements in gas turbine engine systems. Laser-Induced Thermal Acoustics (LITA) is a well understood technique which can make spatially resolved measurements of the local speed of sound, thermal diffusivity, and velocity, from which temperature, pressure, and Mach number may be derived. Of importance for measurements in gas turbine combustors is the ability to make concentration measurements in spray environments. LITA measurements in moderate flow rate simplex sprays are conducted to understand the affects of spray density, ambient pressure, laser energy, and droplet diameter on the percentage of useful individual measurements, or data yield. A Volume Collision and Focusing Model based on kinetic theory is used to predict the variation of data yield with respect to practical spray parameters. Knowledge of realistic gas turbine engine conditions allows for the prediction of the LITA signal to noise ratio at various stations in a nominal gas turbine engine and application of the technique to measurement of component efficiencies and pattern factors.

1 INTRODUCTION

Many traditional optical diagnostic methods for making measurements of thermodynamic and fluid mechanical quantities are appropriate for gas turbine engines. [1] However, the varying conditions and optimization factors of a gas turbine system requires measurement of many parameters (some spatially dependent) within the engine over a wide range of temperatures, pressures and flow conditions. Minimization of the number of individual diagnostics required to examine a functional engine is sought to reduce the measurement setup duration as well as synchronizing and recording data from many different varieties of optical diagnostics (with the attendant amount of data reduction time). Single diagnostics capable of making measurements over the wide-ranging conditions present with similar optical access requirements would have an advantage due to the simplification of the measurement process.

A wide range of optical diagnostics can be applied to gas turbine systems. Researchers have commonly used line-of-sight absorption spectroscopy to measure temperature, pressure, mass flux, velocity, and concentration. [2] While the optical arrangements, data collection, and reliability make absorption diagnostic data simple to quantify, the lack of spatial precision (path integrated measurement) make application of these sensors in the highly three-dimensional engine flows less practical. Also, the requirement of several percent fractional absorption may restrict the measurement to major species in high pressure environments and not be as useful for high bandwidth measurements of emissions.

Isotropic scattering techniques such as Rayleigh scattering allow for spatially resolved measurements of temperature, density, and velocity. However, Rayleigh scattering requires orthogonal optical access to the main optic axis as well as suffers from interference from laser scatter and airborne particles (Mie scattering), which can overwhelm the desired scattering signal in harsh environment. Raman scattering is also an attractive technique for measuring flowfield conditions. In addition to having species specificity allowing concentration measurements, Raman techniques are inelastic affording the ability to spectrally filter the signal. Unfortunately, the main limitation of Raman scattering is a weak signal strength making detection difficult in practical environments. [3]

Laser induced fluorescence (LIF) techniques allow for the spatially and spectrally resolved measurements of all the relevant parameters for gas turbine systems. [4] LIF concentration measurements of major and minor species as well as measurements of temperature, pressure, velocity, and density have been made in a variety of laboratory and practical flows;

---

* Engineer, Member AIAA
† Principal Engineer, Member AIAA
‡ President, Senior Member AIAA

however, dependencies of LIF signals on local excited state quenching rates and rotational energy transfer rates can make measurements difficult to interpret in mixing flows, highly non-uniform flows, or at high pressures.

Techniques based on coherent non-linear optical processes offer several advantages over emission or scattering techniques mentioned previously. The collimated, spectrally narrow signal beams generated by these coherent techniques offer the ability to both spectrally and temporally filter the signal to remove spurious scattered light and natural luminosity, leading to higher signal to noise measurements. [5,6] Also, the ability to remotely detect the coherent beam allows for the placement of higher f# optics away from the experiment, providing shielding from external heat, electrical interference, and other hostile conditions near the sample region. [7]

This paper describes the application of LITA measurements to flowfields relevant to gas turbine engine systems. Prior LITA research is used to estimate the accuracy of the technique over a wide range of conditions and measurement parameters. [8-10] A notable omission from prior experimental research is the ability to make LITA measurements in spray or highly scattering environments. With the optimization of combustor flows highly dependent on spray evaporation and combustion, the ability to make fuel concentration measurements in the spray injection and combustion region is fundamental to the investigation of gas turbine combustors. Highly scattering environments reduce the signal levels as well as act as focusing sites for the pump laser, leading to laser-induced breakdown and signal obfuscation. A model for the data yield in spray environments is posed and evaluated with respect to experimental LITA data recorded in high-pressure spray environments.

2 LITA SIGNALS

A LITA signal is generated by writing a transient grating into a flowfield using a high-power pulsed laser. The decay of the grating reflectivity is then measured by another laser beam. The probe volume can acousto-optically respond to this forcing by mainly thermalization or electrostriction at conditions internal to gas turbine engines. Both electrostriction and thermalization produce density perturbations in the sample volume. The magnitude of electrostriction is proportional to the real part of the susceptibility of the sample gas (c.f. index of refraction). The magnitude of thermalization is proportional to the negative imaginary part of the susceptibility (i.e., absorption coefficient) [11]. Because of the different physical mechanisms of these optoacoustic effects, the signals they produce are readily distinguished. Electrostriction produces ringing at twice the Brillouin frequency of the grating and thermalization produces ringing at the Brillouin frequency [12]. The time evolution of the signals can be understood in terms of the superposition of density fields of the thermal grating and counter-propagating acoustic waves. The ringing frequency is related to the local speed of sound, while the decay of the LITA signal is proportional to the thermal diffusivity. Thus, if the gas composition is known, accurate measurements of both temperature and pressure is possible in a single-shot manner.

One strength of LITA is the ability to make physical measurements without using spectroscopic information. However, both components of the complex linear susceptibility of the sample gas can be measured from LITA signals. The ratio of the species-resonant imaginary component (absorption and thermalization) to the non-resonant real component (electrostriction) provides a self-referenced measure of the absolute resonant species concentration [13]. This measurement is independent of laser power fluctuations and background noise sources. LITA also possesses higher sensitivity than other ratiometric techniques, e.g., Broadband CARS. The ability to make accurate concentration measurements requires that the electrostrictive and thermal grating signals be of the same order of magnitude. Concentration measurements in spray environments are straightforward as long as the spray induced breakdown and scattering is small enough to allow a non-zero data rate.

3 BASIC DESCRIPTION OF GAS TURBINE COMPONENT SYSTEMS

A schematic of a typical gas turbine engine is shown in Figure 1. The main elements of this type of propulsion system are the inlet, compressor, combustor, turbine, and nozzle. Other elements such as afterburning, inlet fan, and bypass streams are present in many modern gas turbine engine designs. However, the discussion of LITA signal measurements in gas turbine systems requires only the examination of the basic components and their thermodynamic conditions.

Inlets provide incoming air to the compressor or fan at the highest stagnation pressure possible with minimum spatial variation in stagnation temperature and pressure. For subsonic inlets, this requires measurement of separation at extreme angles of attack and minimization of drag penalties at high air demand. While the static pressure is nearly constant at the compressor face, the stagnation pressure (and thus the velocity) can vary spatially due to wall friction and

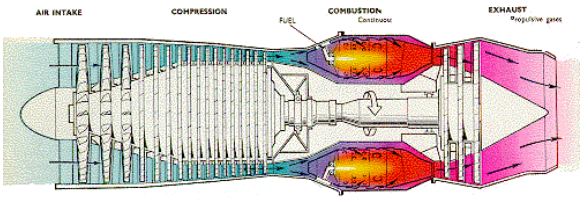

Figure 1 Schematic of gas turbine engine. http://www.aircraftenginedesign.com.

separation. This distortion will cause the rotor blade to encounter a sudden increase in angle of attack, which can lead to stall and compressor surge. [14]

Axial compressors present in most gas turbine engine systems perform nearly adiabatic work on the incoming airflow, raising the stagnation pressure. The close packed system of rotor and stator blades make optical access very difficult to measure inter-stage properties without a specially modified engine. Thus, only measurement of compressor exit quantities is most likely possible. Measurements of the local stagnation pressure and temperature as well as Mach number allow for estimation of the local compressor polytropic efficiency and gain coefficient of the inlet distortion field. The latter is useful in determining a potential source of combustor instability.

Gas turbine combustors represent an extremely harsh environment in which to make measurements. The extremely high pressures and temperatures often hamper the accuracy of many diagnostic tools. The combustor is heat addition at nearly constant pressure. However, many complicated physical processes in the combustor chamber must be quantified for optimum performance. Following the initial diffuser stage, fuel atomization, evaporation, and mixing occurs prior to ignition. Dilution air is then added through liner holes in the intermediate and dilution zones. This mass addition is used to promote efficient combustion and minimize pollutant formation as well as to generate a suitable pattern and profile factors prior to entry into the turbine stages of the engine. [15] All of these processes also play a role in combustor stability through the interaction of pressure oscillations with the primary reaction zone.

The turbine operates similarly to the axial compressor mentioned above, with the exception that many of the initial high-pressure stages may be actively cooled. Optical measurements of inter-stage processes are again hampered by limited optical access in practical systems. However, at the turbine exit, spatially precise estimation of turbine polytropic efficiencies as well as multi-stream flow losses is useful for improved design. Finally, afterburning is common in military gas turbine combustion systems.

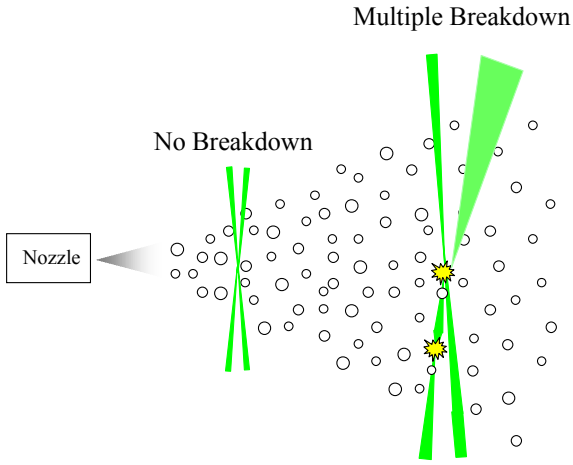

Figure 2 Cartoon of LITA measurements in sprays, including situations of both good signal generation and spray-induced breakdown.

Ducted burning of injected spray fuels also allows for mixing, combustion efficiency, and pollutant measurements to be made in both turbofan and turbojet engines.

4 LITA Data Yield Model in Spray Environments

LITA signals have been evaluated at many of the conditions present in gas turbine engines, as described above. However, there exists limited experimental data on the ability to make LITA measurements in spray environments. The data yield of LITA experiments in spray environments will be limited by the collision and focusing effects of droplets in the flowfield (Figure 2). A simple Volume Collision and Focusing Model (VCFM) is formulated in order to determine the effects of various experimental parameters on the percentage of useful LITA signals. "Useful" signals are those which both a frequency (speed of sound) and decay (thermal diffusivity) can be measured accurately. Using a kinetic theory type approach [16], the number of collisions that a laser beam might encounter when traveling through a spray is shown in Equation 1.

$$N_{coll} = 2\pi \int_{-R_{spray}}^{R_{spray}} n_{spray}(r,\theta,z)\left(r_{las}(r) + R_{drop}(r,\theta,z)\right)^2 dr \qquad [1]$$

where n_{spray} is the number density of droplets within the spray as a function of position, r_{las} is the HWHM of the laser beam intensity, R_{drop} is the size of the colliding droplet, and the coordinate system is fixed at the origin of the spray nozzle. The number of collisions is expressed as a probability as the laser propagates from across the entire spray (Figure 3). The size of the droplet relative to the size of the beam determines both

the scattering cross section (for low power beams) and beam focusing (for high power beams). Thus the number of detrimental collisions can be expected to scale as Equation 2,

$$N_{coll\_eff} \propto 2\pi \int_{-R_{spray}}^{R_{spray}} A_{eff}\, n_{spray}(r,\theta,z)\left(r_{las}(r) + R_{drop}(r,\theta,z)\right)^2 dr \qquad [2]$$

$$\text{where } A_{eff} = f\left(r_{las}, R_{drop}, \theta_{drop}, V_{BD}, \lambda, I_{las}, SNR\right)$$

where A_{eff} represents a collision effectiveness parameter. This parameter depends on the particulars of each laser/droplet interaction as well as the local laser intensity (I_{las}) and local breakdown voltage (V_{BD}) of either the liquid or gaseous phase. If a collision occurs, the relative sizes of the beams and droplets along with the laser power and interaction angle determine whether the collision is of the scattering or focusing plus scattering type [17]. The particulars of each collision can be treated using Mie scattering theory, but are not formally treated in this analysis. Internal refraction of laser light (Figure 4) causes focusing of the transmitted wave through the droplet. Geometrical optics can be used to calculate the beam paths for finite intensities (as the beam diameter is much greater than the diffraction spot size); however more complete theory involving the focusing of Gaussian laser beams is required to describe the true laser power at the focused location. The particulars of the beam focusing and subsequent laser scattering or laser-induced breakdown are beyond the scope of this effort. However, characterization of the results gained in this study is performed using the form of Equation 2.

In order to predict the approximate data loss due to focusing and laser-induced breakdown, Equation 2 was simplified to Equation 3 by assuming a mono-disperse spray (at the SMD), uniform droplet distribution within the spray boundaries, and using a spatial average laser beam diameter along the spray diameter. A_{eff} is assumed to be constant throughout the spray region as the beam diameter and spray droplet diameter are fixed.

$$N_{coll\_eff} = 2\pi A_{eff}\, n_{spray}(z)\left(w_{las} + R_{SMD}\right)^2 L_{spray} \qquad [3]$$

A_{eff} is assumed to scale as $1/I_{las}$ due to reduced power at the laser focus and with SNR due to difficulty

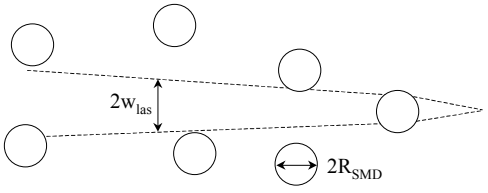

Figure 3 Schematic of Volume Collision and Focusing Model, similar to that of a mean free path in gas kinetic theory.

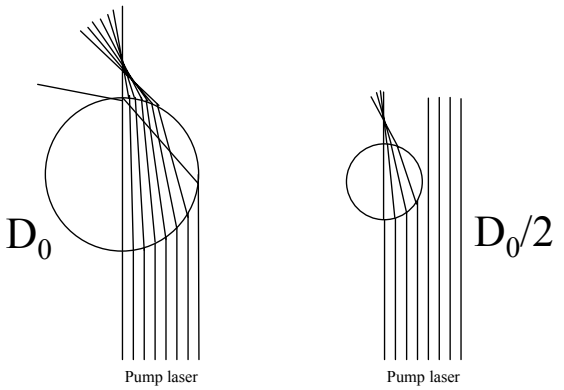

Figure 4 Focusing of incoming light rays by water droplets in air. Larger droplets subtend more of the light as well as create a tighter focus.

fitting the LITA signal for both speed of sound and thermal diffusivity information, as will be discussed later.

The data yield from the LITA experiments is directly related to the number of detrimental collisions the source and signal beams encounter while propagating through the medium. Thus, the average data yield at a spray condition will be the probability of not colliding with a focusing droplet. This is simply stated in Equation 4.

$$\text{Data Yield} = 1 - N_{coll\_eff} \qquad [4]$$

However, the data yield likely does not go to zero at the origin of the spray due to misalignments between the spray centerline and grating plane, liquid sheet formation and breakup (dissimilar focusing properties as compared with individual droplets) near the spray nozzle, and large variations in the local droplet sizes (high anisotropy) prior to shattering and coalescence. Thus a non-zero data yield is expected close to the spray nozzle and must be added in as an adjustable constant (C_0).

$$\text{Data Yield} = 1 - N_{coll\_eff} + C_0 \qquad [5]$$

5 EXPERIMENTAL SETUP

The LITA system used for these measurements and has been developed by Advanced Projects Research, Inc. as a commercial product. Briefly, a high power Nd:YAG laser (532 nm) acts as the driver laser, creating the grating in the probe volume. The probe laser, an Ar^+ laser operating at 488 nm, is also focused into the probe volume and generates the signal beam as it coherently scatters off the transient grating. The

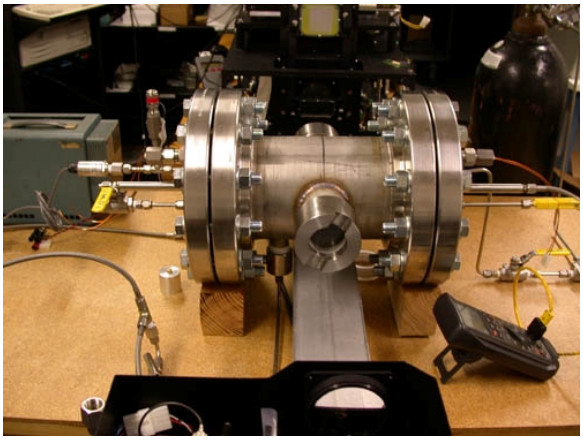

Figure 5 Image of high-pressure spray facility with optical access aligned with the LITA measurement direction.

forward phase matching, four-beam crossing geometry is similar to CARS experiments. The LITA system also contains a calibration leg of exactly similar dimensions as the probe volume. Performing LITA in a known environment as a calibration allows for the determination of beam sizes and crossing angles directly from experimental data. The signal beam is recorded using a PMT masked with a spatial filter to increase the spatial resolution and noise rejection of the system. The LITA system spatial resolution including the masking pinhole is solid cylinder 200 μm in diameter and 1mm in length.

LITA measurements are made in a high-pressure bomb with optical access. The bomb and associated plumbing is shown in Figure 5. The optical access is provided by opposed 5 cm diameter glass windows, which are spaced 25 cm apart.

The large separation of the windows with respect to the main body was created in an effort to minimize laser damage to the window surfaces from focused high power YAG beams. Either single spray or opposed spray nozzles can be examined in this facility. Furthermore, the spray nozzles may be translated through the test section by the use of a simple shaft seal on the liquid delivery system. Total water flow and LITA run time was limited by the pressure rise in the test section due to the addition of mass by the spray. Thus, test times were restricted to 30 sec at 0.25 GPM (gallons per minute) to limit the pressure rise to 2%. The tank was pressurized with dry nitrogen to minimize any minor absorbing species concentrations. The LITA system and receiver are shown in the background and foreground of Figure 5, respectively. Figure 6 shows the simplex atomizers used in this study. The brass nozzles pictured are simple solid cone atomizers, with the smaller optimized for the creation

Figure 6 Image of three types of pressure simplex atomizers examined in this study. The larger, solenoid controlled nozzle is an automotive spray injector.

of fine mists. The larger, solenoid operated nozzle is of an automotive type but had too small a flow rate for use in this study.

6 RESULTS

6.1 Data Yield Measurements in High Pressure Sprays

A comparison of two separate nozzles was performed to examine the differences in data yield for a large change in flowrate and SMD. Nozzle 1 is the a 0.25 GPM pressure swirl, simplex atomizer with a typical SMD ~ 120 μm. SMD estimation is performed using correlations from [15, 20]. A second nozzle operated in a similar pressure range but at much lower flow rates was used to examine the effects of a smaller SMD. Nozzle two was of the misting atomizer type and had a flow rate of 0.06 GPM. Its nominal droplet size is estimated to be ~50 μm using the stated specification

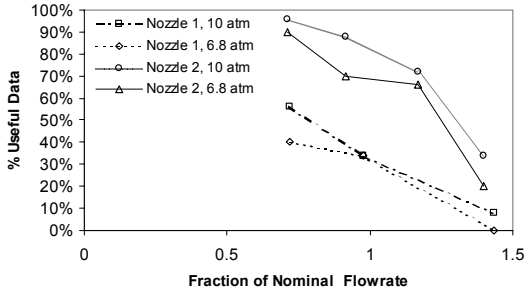

Figure 7 Comparison of the single-shot LITA signal data yield from two different nozzle types with respect to variation in the total flowrate and ambient pressure. Nozzle 1 is a 0.25 GPM pressure simplex atomizer; Nozzle 2 is a 0.06 GPM misting atomizer.

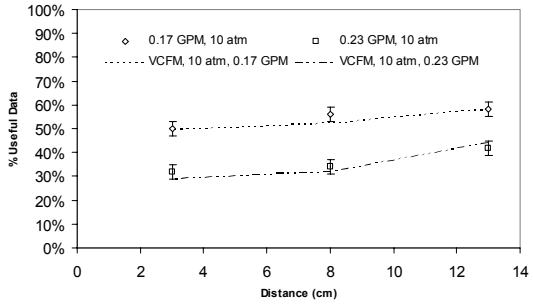

Figure 8 Single-shot LITA data yield at 10 atm with variation in downstream distance from a full cone, 0.15 GPM pressure simplex atomizer.

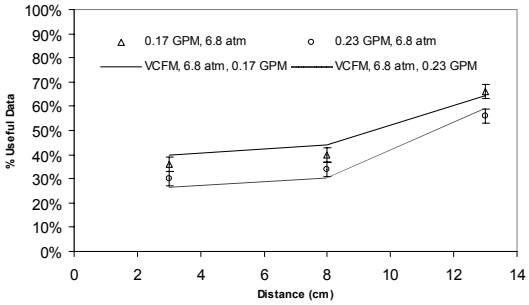

Figure 9 Single-shot LITA data yield at 6.8 atm with variation in downstream distance from a full cone, 0.15 GPM pressure simplex atomizer.

scaled for the ambient conditions and inlet pressures used. The LITA signals were recorded at the middle downstream location (8 cm) and at 10 atm. The flow rate was varied from 60 to 140% of the nominal flow rate for each of the two nozzles. The comparison between the two nozzle types are shown in Figure 7. Due to the much smaller SMD of the misting nozzle (Nozzle 2), a smaller number of breakdown collisions are expected. While the lower flowrate nozzle had a smaller overall flowrate, it had a much larger droplet density due to its atomization technique. The spray angle was held constant between the two nozzles ($\theta \sim 45^{o}$ at 10 atm), as well as the collisional path length. At the reduced mean droplet diameter, the data yield is much higher, approaching 100% at 60% of the nominal flowrate.

This scaling of the data yield of the second nozzle can be illustrated by comparing the spray characteristics to that of the first nozzle. The smaller droplets of the misting spray will subtend less of the pump beam, and thus focus less of the optical energy. Secondly, the smaller droplets cannot produce as tight of a focus due to higher interface curvature and spherical aberration (Figure 1). Consequently, the smaller diameter droplets more greatly scatter rather than focus the incident laser radiation. This results in lower overall signal levels, as pump, probe, and signal beams are all attenuated as they propagate through the spray environment. As the inlet pressure and flow rate of the misting nozzle is increased to the nominal value, the droplet density increases and the large droplets from the distribution act to focus the pump laser to breakdown intensity. As the misting nozzle is operated at yet higher pressures, the data yield drops precipitously. Droplet coalescence along with high droplet densities cause larger droplets to be created and more pump laser energy to be focused.

The volumetric collision and focusing model (VCFM) is used to describe the general trends of the LITA data yield with respect to position within the spray cone, injection pressure, ambient conditions, and driver laser power. These trends are shown in Figure 8-10. Figure 8 details the variation of LITA data yield with spray location and nozzle flow rate at 10 atm. Fifty LITA signals are recorded for each condition and the data yield again consists of the percentage of LITA data traces which allow for accurate single-shot measurements of both the speed of sound and the thermal diffusivity. For the speed of sound measurement, errors less than 2.2% with respect to the average value are allowed (an error of 5% for the temperature). While for the thermal diffusivity measurement, errors less than 10% are tolerated. These represent reasonable data variation for the single-shot LITA traces while still allowing for very accurate ensemble averaged data sets to measure the mean properties (< 0.3% for speed of sound and < 1.5 % for the thermal diffusivity).

The data yield at 10 atm slowly increases with downstream distance. As the spray develops and entrains more ambient air, the droplet density decreases, allowing for fewer focusing events. The collision model accurately represents the data yield trends along the spray centerline. Radial traverses were not possible due to the viewing limitations placed by the optical access. The constant in Equation 5 was fixed to provide the most accurate fit of both flowrate data, and the constant $A_{eff} = 0.2$ was used for both flowrates. Droplet distributions and spray number densities were computed using validated correlations for simplex atomizers.

The correlation of the VCFM with the experimental data at 6.8 atm is not as good (Figure 9). However, the general trend of increasing data yield with downstream distance is again present. At this lower pressure, a uniform droplet distribution takes longer to develop with larger droplets existing near the spray nozzle. Thus, a larger increase is seen in the data yield at the furthest downstream location due to the

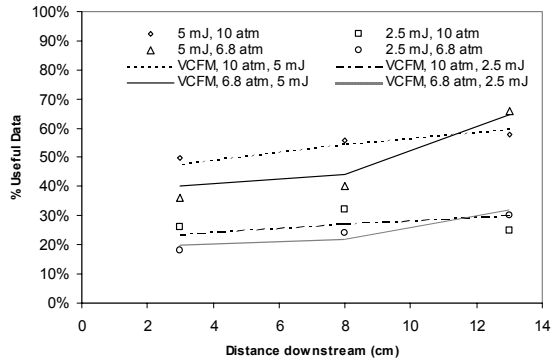

Figure 10 Comparison of single-shot LITA data yield in 10 atm and 6.8 atm spray environments with variation in the pump laser energy. Spray is a full cone, pressure simplex atomizer at 0.15 GPM, 13 cm downstream of the nozzle.

complete breakup of the initial liquid sheet. Again the variable constant in Equation 5 was chosen to best fit each data set, the constant $A_{eff} = 0.27$ was used for both flowrates. The increase in the break down effectiveness as the ambient pressure decreases is expected as the SMD of simplex atomizers is a weak function of pressure. As the pressure decreases, the SMD increases, causing more energy of the incoming pump beam to be focused.

Reasons behind the reduced correlation at the lower pressure condition are not completely clear. At the lower pressure, the liquid sheet breakup and normalization of the droplet distribution occurs further downstream and can cause variation in the droplet size as a function of downstream distance. Also, the lowered pressure reduces the overall LITA signal, which can cause poor signal fitting if the SNR of the single-shot data is insufficient to render thermodynamic property measurements within the allowable error bounds. The lowered SNR coupled with potential scattering from smaller droplets can significantly reduce some single-shot signal levels, creating much higher data yield variability.

When fitting the simple model to the experimental data with variation in the driver laser energy, the basic scaling of $\sim I_{las}$ applies fairly well (Figure 10). Laser power quoted is the total laser energy in both pump beams. As the laser power is decreased, the ability of the focused laser to cause breakdown decrease linearly. Thus, the data yield should increase linearly with decreasing driver laser power if only focusing is considered. However, the LITA signal depends on the square of the driver laser energy and the data yield also depends on the SNR. Low SNR data sets are unable to be accurately fit to extract precise values for the thermal diffusivity or the speed of sound. If the data yield is assumed to be linear in the single-shot SNR over the current signal level regime (SNR = 3 – 20), then the data yield scales inversely with laser power, as shown in Figure 10. Here the laser power was reduced by a factor of two, and the average data yield also decreased by the same factor. However, the greater deviation seen in the lower power results is likely due to enhanced noise levels and greatly decreased SNR.

6.2 Characteristic LITA Signals

This section describes the character of the optical signals generated during LITA measurements in spray environments. All of these results were taken with the LITA system in the high-pressure spray facility, both previously described. Figure 11 details a single-shot LITA measurement in a high-pressure spray environment, taken 13 cm downstream of a 0.15 GPM simple nozzle. The theoretical fit shows excellent agreement with the instantaneous signal, which has a single-shot SNR of 7. This allows extraction of the local speed of sound and thermal diffusivity, which differ from their accepted values by 0.4% and 6% respectively. Higher accuracy in the thermal diffusivity measurement requires compensation for potential beam misalignments in the test section due to stress-induced birefringence in the windows as well as differential refraction of the pump and probe beams [21]. However, ensemble averaging of this type of LITA signal along with precise monitoring of beam misalignments with changing test section pressure would allow for higher accuracy measurements of these quantities.

Interesting effects occur when laser focusing and breakdown occur near the measurement volume. If the breakdown event occurs well before the measurement

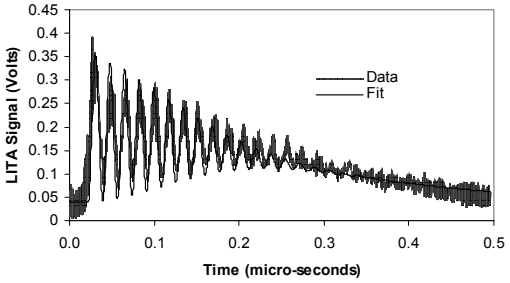

Figure 11 Single-shot LITA signal at P = 10 atm, simplex atomizer spray at 0.17 GPM, 13 cm downstream of nozzle, I_{las} = 5 mJ. Speed of sound = 343 m/sec, D_{th} = 0.0175 cm^2/sec.

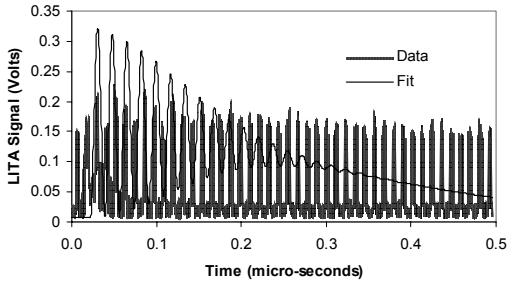

Figure 12 Single-shot LITA signal with significant air breakdown. Data shows a uniform intensity in time with a ringing frequency at 87 MHz, exactly three times the local Brillouin frequency. Electrostriction signals show ringing at twice the local Brillouin frequency, 58 MHz.

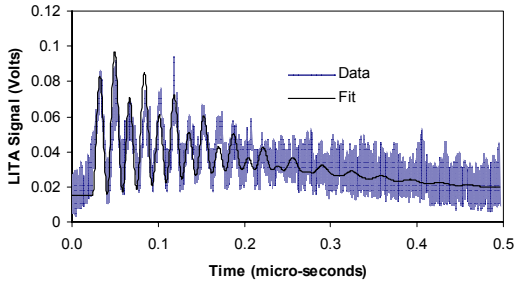

Figure 13 Single shot LITA signal exhibiting absorption from breakdown region. Signal level is attenuated and significant laser absorption in room air has occurred due to enhancement of every second peak (thermalization signature). P = 10 atm, simplex atomizer spray at 0.17 GPM, 13 cm downstream of nozzle, I_{las} = 2.5 mJ.

volume, then only a weak signal from the scattered pump and probe beams is seen for the duration of the breakdown event with no ringing component. As the breakdown approaches the measurement volume, the affects of the perturbation to the local air properties and LITA signal can be seen. Figure 12 shows an example of the LITA signal recorded simultaneous with a breakdown event. The generated signal bears no resemblance to the fitted signal (similar to that from Figure 11). In fact, the signal here is uniform in peak intensity with time with a ringing frequency that is three times the unperturbed Brillouin frequency. This effect is potentially due to the local heating of the gas by a factor of 2.25, which would increase the frequency of the density field modulation by a factor of 1.5. Then acoustic wave packets traveling away from each other would have a similar frequency spectrum. However, there appears to be no significant decay of this signal over the usual LITA interrogation times as well as little frequency chirp (which would be associated with the cooling of the probe volume). Thus, it is unclear at this time what effect the local breakdown conditions have on this LITA signal.

Another LITA signal recorded simultaneously with a breakdown event is shown in Figure 13. Here a significant thermalization as well as electrostriction signal is present in pure nitrogen. The breakdown event has caused local absorption and thermalization of pump laser photons, creating a thermal grating where initially no absorbing species existed. This type of data trace, though rarely seen, is a great concern when making concentration measurements, as the induced thermalization signal from the breakdown event can be easily mistaken for a true thermalization signal which would be used to calculate absolute concentration levels. Acoustic or optical breakdown monitors in the test section could eliminate the recording of these spurious LITA signals.

Variation in the test section pressure or laser energy alters the generated LITA signal as expected. Figure 14 shows the LITA signal at 6.8 atm. The signal has a slightly lower intensity and signal to noise ratio, but the fitting routines allow for similar accuracy in the fitting of parameters as Figure 11. Figure 15 shows the LITA signal at 10 atm with reduced laser intensity. Again the character and fitting of the data are similar to previous results, though the SNR is further reduced.

Finally, the effects of scattering from small droplets contained in a fog are seen in Figure 16. In order to generate the LITA data sets the spray nozzles were run for 30 second intervals into a closed chamber. For the larger SMD spray nozzle, this resulted in a pooling of liquid at the bottom of the test section. However, for the misting spray nozzle, a dense fog was created over time. This fog did not often induce breakdown, but rather attenuated the pump, probe, and signal beams as they propagated through the test facility. LITA signal attenuation levels of up to 80%

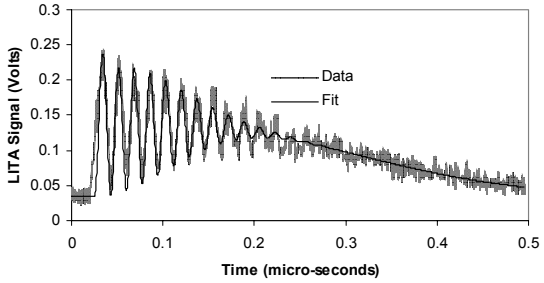

Figure 14 Single-shot LITA signal at P = 6.8 atm, simplex atomizer spray at 0.17 GPM, 13 cm downstream of nozzle, I_{las} = 5 mJ. Speed of sound = 343 m/sec, D_{th} = 0.026 cm^2/sec.

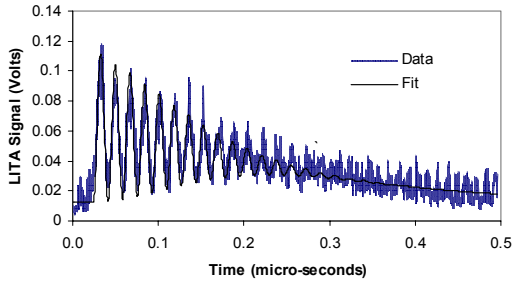

Figure 15 Single-shot LITA signal at P = 10 atm, simplex atomizer spray at 0.17 GPM, 13 cm downstream of nozzle, I_{las} = 2.5 mJ. Speed of sound = 343 m/sec, D_{th} = 0.018 cm^2/sec.

were seen with this nozzle without breakdown, though due to the relatively high SNR of these measurements, thermodynamic parameters could still be extracted from this attenuated data.

7 Discussion of LITA Measurement in Gas Turbine Components

Both analytic and experimental correlations for signal strength with varying thermodynamic conditions are used to determine the potential SNR of LITA measurements in gas turbine engines. These include the relative contributions in signal from population, thermal, and electrostrictive gratings, as well a noise from beam steering and density gradients

Population gratings in LITA or DFWM experiments have severe pressure scaling (~ P^{-6} in the homogeneously broadening limit and ~ P^{-4} in the Doppler broadened regime). [7]. As the pressure and thermalization (collisional quenching rates) increase, the relative strength of population gratings decreases, and thermal and electrostrictive gratings come into prominence. [22] Thermal gratings intensity increases slightly with increasing density and decreases quadratically with increasing pressure, while electrostrictive gratings increase linearly with density and decrease linearly with temperature (at fixed pressure). These scaling laws assist in determining LITA signal levels and potential SNR at various conditions within the gas turbine system.

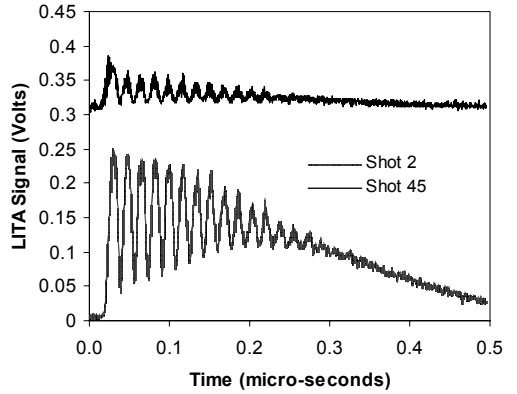

Figure 16 Single-shot LITA signal at P = 10 atm, misting atomizer spray at 0.06 GPM, 13 cm downstream of nozzle, I_{las} = 10 mJ. Saturated fog increased scattering losses in the test section over time. Shot 45 occurred 22 seconds after shot 2.

Of concern in practical high pressure systems is beam steering by high intensity turbulence or large density gradients within the flow. Strong beam steering effects can be minimized by propagating the beams perpendicular to contours of constant density. [1] However, the forward phase matching geometry used in this LITA system has small crossing angles, and thus the three beams entering the flowfield pass through similar density gradients. Also, finite beam effects and Doppler beating are important as the observation time is sufficiently long to allow the generated acoustic energy to leave the grating volume. This Doppler beating can limit the ability to make accurate measurements of the thermal diffusivity at very high pressure conditions as finite beam size effects increase with increasing pressure. [23]

Using the previous results and analysis along with prior LITA research and experiments, estimates for the effectiveness of LITA to make measurements in gas turbine engine components can be formulated. A low bypass ratio two-spool gas turbine engine for military is assumed for use as the target system for measurement: A nominal afterburning engine a bypass ratio of 0.75, a compressor pressure ratio of 25 and a fan pressure ratio of 3. Component efficiencies and operating parameters are assumed to fall within the typical ranges.

Table 1 Estimated thermodynamic quantities at various locations in a military, low-bypass ratio, turbofan engine

Position	T (K)	P (atm)	Mach No.	Rel. Density
Inlet	288	1	0.45	1
Post Fan	425	3	.25	2
Compressor	850	25	.15	8.3
Primary Comb.	2100	25	.4	3.4
Post Combustor	1600	23.5	.3	4.2
Post Turbine	800	3	.4	0.7
Exhaust	640	1	.8	0.45

7.1 Inlet System

Standard density means relatively weak electrostrictive signals. Single-shot heterodyne LITA velocimetry has been shown to be possible at these velocities and conditions using a higher power probe laser. Slight seeding of the incoming air with NO_2 (1 ppm such as on a smoggy day) would increase the SNR of this data by a factor of 10. However, good agreement with pitot probe data (< 0.2%) was achieved with heterodyne LITA in unseeded air at 150 m/sec [10]. Measurements of this accuracy could be used to quantify both the turbulence and inlet distortion accurately.

7.2 Fan/Compressor

The increased density of the flow means that the electrostrictive signal to noise will increase by a factor of 1.6 behind the fan and a factor of 5 after the compressor, assuming a constant level of background scatter and beam steering. These higher signal levels allow for very accurate measurement of the temperature, pressure, and velocity at these engine stations using heterodyne LITA measurements. The spatial resolution also allow for good estimation of the flow distortion and turbulence entering the combustor.

7.3 Combustor

The first section of the combustor, the spray evaporation zone, occurs at high pressure and elevated temperatures. Previous research has shown that concentration measurements from the relative intensity of electrostrictive and thermal gratings has provided high accuracy (<3%) absolute concentration measurements of a seeded tracer. If the tracer has similar a similar boiling point or distillation as heavy aircraft fuels, then it will be an accurate marker of fuel concentration in the pre-flame region. These measurements were made at both atmospheric and elevated pressures at constant temperature. Scaling these results using the closed form solution of the LITA signal strengths [12] provides an estimate of the accuracy of these measurements. Many potential choices for the tracer molecule exist and would be chosen taking into account available laser sources and matching of its boiling point to nominal jet fuels. The ratio of the electrostriction to thermalization energy densities scales nearly linearly with density ($\sim PT^{-1.2}$) The expected SNR of absolute concentration measurements of evaporating droplets at the post compressor location is 15 (similar to that of the atmospheric pressure experiments) decreasing to 10 near the flame base, using the a scaled results from [19]. This measurement accuracy would allow for mapping of the entire concentration field in the spray region.

The prior analysis assumed no attenuation of signal or loss of data yield to due to droplet scattering and focusing as discussed in section four. Using the information gained in this experimental effort coupled with the known droplet characteristics of some airblast atomizers is gas turbine systems, a prediction of data yield in gas turbine spray systems is possible. Typical piloted airblast atomizers have high droplet densities near the edges of the spray cone along with droplets evenly distributed near the spray core, thus decreasing the effective collisional path length (Equation 1). Airblast atomizers also have a smaller droplet SMD over a wider range of injection pressures and conditions, which would increase the data yield through both the droplet size and focusing power (A_{eff}). However, the droplet densities are much higher in the edges of the spray than in the full cone simplex atomizers examined in this study, which would tend to decrease the data yield sharply at those spatial locations. The accumulation of all of these effects makes prediction of the exact data yield difficult as the spray characteristics vary widely over all the atomizers in use in gas turbine engines today. However, the VCFM has shown to be a useful tool in estimating the ability to make predictions of LITA signal data yield, and thus can be applied to any particular engine configuration.

7.4 Combustion zone

The high pressure of gas turbine combustors alleviates the typical difficulty of making LITA measurements in combustion environments. In atmospheric pressure flames, the large volumetric expansion reduces the quenching and thermalization rates greatly reducing the intensity of thermal gratings. Also, the low pressure and high temperatures severely attenuate the production of electrostriction gratings. Previous researchers have used other grating mechanisms such a population and polarization gratings to produce scattering environments at these low density conditions. However, from Table 1, the density in the gas turbine combustor is more than an order of magnitude greater than typical laboratory flame conditions, allowing for the strong production of both electrostrictive and thermal gratings (if the pump laser is tuned to an appropriate tracer transition). This permits accurate measurement of both the speed of sound and thermal diffusivity throughout the highly self-luminous flame environment. Temperature and pressure measurement accuracy here is hampered by

the uncertainty in the gas composition. However, reasonable bounds may be placed on the ratio of specific heats and mixture gas constant using lean combustion chemical simulations.

7.5 Turbine

The increase in engine efficiency and power over the past 50 years of gas turbine research can be partially attributed to improvements in turbine technology through new materials, active cooling, and new geometry capabilities. Of great importance to the effective operation of modern axial turbine systems is the quantification of the spatial variation in temperature just prior to entry into the first stage of the high-pressure turbine. This variation is known at the pattern factor or turbine profile factor, which is a measurement of the temperature deviation from the desired profile. Using a LITA measurement system with its high spatial resolution, this profile factor can be easily measured and be used to assist the optimization of the combustor exit temperature profile as well as gas mixing in the dilution region of the combustor.

Regions after the turbine exit pose the greatest difficulty for LITA measurements. The low-density conditions just after the turbine as well as the extremely low densities just after the afterburner severely inhibit the creation of thermal and electrostrictive gratings. LITA signal SNR for the post turbine region using the existing setup would be just greater than unity and in the afterburner region would be $<< 1$. Higher pump and probe lasers coupled with high seeding densities and reduced grating crossing angles could be used to alleviate this loss in signal; however, this would result in higher breakdown potential as well as reduced spatial sensitivity.

Alternatively, measurements in these locations using the current LITA system would require the use of population gratings and the seeding of flows with relatively large levels of absorbing species. One possible tracer species is nitric oxide (NO) as it is already present in the effluent stream of the combustor. However, with modern gas turbine systems operating at very low NO_x production levels, sufficient signal intensity may be difficult to achieve without augmentation of the stream with further NO. This presents a safety hazard as well as can alter the operation of the engine. Also, the probe beam of the system would need to spectrally match the pump beams (as in DFWM) for further enhancement of the signal. Thus, optical measurements of thermodynamic quantities after the turbine exit would require other optical techniques which are more suited to making measurements in near atmospheric flames (CARS, LIF, or pulsed DFWM using population gratings). These diagnostics could be used in conjunction with LITA measurements upstream of the turbine exit to well characterize the flow field through a gas turbine engine.

8 CONCLUSIONS

The application of LITA to make optical measurements in gas turbine engines was examined. Spatially resolved concentration measurements in a fuel spray environment are desired to complement other measurements possible using LITA. A high-pressure spray facility was constructed to mimic the near field spray environment of a gas turbine engine system. The operating density range of the facility was matched to modern gas turbine compressor exit conditions. The percentage of useful single-shot signals was explored over a range of ambient conditions and LITA measurement parameters. Laser-induced breakdown and scattering losses were seen to cause a reduction in data yield of the measurements in regions of large droplets and high spray droplet density. A Volume Collision and Focusing Model based on kinetic theory was developed and evaluated with respect to the experimental data. Agreement between the model and experimental trends was good over the variation of several parameters.

The LITA signal to noise ratio and measurement applicability to gas turbine components is estimated for a low bypass-ratio military afterburning engine. Measurements of local velocity, temperature and pressure are possible in the engine inlet and compressor to estimate both polytropic efficiency and pattern factor. LITA signal estimates were also made in the combustor zones: spray injection and evaporation, primary reaction, and dilution regions. Accurate measurements of local temperature, pressure, fuel and emissions concentrations, and turbine profile factor are possible due to the elevated pressure at which combustion occurs. This high pressure and density enable the efficient generation of thermal and electrostrictive gratings. Precise LITA signals in the post turbine and afterburner regions of the engine are shown to suffer from very low SNR. Measurements at these locations would likely require the use of alternative optical measurement techniques.

9 ACKNOWLEDGEMENTS

The authors would like to thank Advanced Projects Research, Inc. for sponsoring this research as well as

Keith Robinson for his assistance in the design and construction of the high pressure spray facility.

10 REFERENCES

[1] Eckbreth, A.C. (1988) *Laser Diagnostics for Combustion Temperature and Species*, Abacus Press, Cambridge, MA.

[2] Hanson, R.K., Baer, D.S., Morris, C.I., Thurber, M.C., Furlong, E. and Wehe, S.D. (1999). "Recent Advances in Laser-Based Diagnostics for Gaseous Flows," *J. Visualization*, Vol. 2, No. 3.

[3] McEnally, C.S., Pfefferle, L.D., Schaffer, A.M., Long, M.B. Mohammed, R.K., Smooke, M.D., and Colket, M.B. (2000) "Characterization of a Coflowing Methane Air Nonpremixed Flame with Computer Modeling, Rayleigh-Raman Imaging, and On-Line Mass Spectrometry," *Proc. Combust. Inst*., Vol. 28, pp. 2063-2070.

[4] Hanson, R.K., Seitzman, J.M., and Paul, P.H. (1990) "Planar Laser-Fluorescence Imaging of Combustion Gases," *Appl. Phys. B*, **50**, pp. 441-454.

[5] Brown, M.S. and Roberts, W.L. (1999) "Single Point Thermometry in High-Pressure Sooting, Premixed Combustion Environments," *J. Propulsion Power*, **15**, pp. 119-127.

[6] Williams, S., Rahn, L.A., Paul, P.H., Forsman, J.W., and Zare R.N. (1994) "Laser-induced Thermal Grating Effects in Flames," *Opt. Lett*., **19**, pp. 1681-1683.

[7] Danehy, P.M. (1995) *Population and Thermal Grating Contributions to Degenerate Four-Wave Mixing*, Ph.D. Thesis, Stanford University.

[8] Baker, P.F., Grinstead, J.H. and Miles, R.B. (1999) "Single-Pulse Temperature Measurement in Supersonic Air Flow with Predissociated Laser-Induced Thermal Gratings," *Optics Comm.*, **168**, pp. 177-182.

[9] Schlamp, S., Cummings, E.B., and Sobota, T.H. (2000) "Laser-Induced Thermal-Acoustic Velocimetry with Heterodyne Detection," *Opt. Lett.*, **25**, pp. 224-226.

[10] Hart, R.C., Balla R.J., and Herring, G.C. (1999) "Nonresonant Referenced Laser-Induced Thermal Acoustics Thermometry in Air," *Appl. Opt.*, **38**, pp. 577-584.

[11] Eichler, H. J., Gunther, P. G, and Phol, D. W. (1986) *Laser-Induced Dynamic Gratings*, Springer-Verlag, New York.

[12] Cummings, E. B. (1995) *Laser-Induced Thermal Acoustics*, Ph.D. thesis, California Inst. of Technology, Pasadena, CA.

[13] Schlamp, S. and Sobota, T.H. (2002) "Measuring Concentrations with Laser-Induced Thermalization and Electrostriction Gratings," *Exp. Fluids*, Vol. 32, pp. 683-688.

[14] Oates, G.C. (1985) *Aerothermodynamics of Gas Turbine and Rocket Propulsion*, AIAA Education Series, New York, NY.

[15] Lefebvre, A.H. (1999) *Gas Turbine Combustion*, Taylor and Francis Inc., Philadelphia, PA.

[16] Vincenti, W.G. and Kruger, C.H. (1977) *Introduction to Physical Gas Dynamics*, Kreiger Publishing Co., New York, NY.

[17] van de Hulst, H.C. (1957) *Light Scattering by Small Particles*, Dover Publications, New York, NY.

[18] Schlamp, S. (2000) *Laser-Induced Thermal Acoustic Velocimetry*, Ph.D. Thesis, California Institute of Technology.

[19] Rossmann, T., Moore, K. C., and Sobota, T. H. (2002) "Simultaneous PLIF and LITA for Absolute Two-Dimensional Concentration Measurements in Turbulent Mixing Flows," 22nd AIAA Aerodynamic Measurement Technology and Ground Testing Conference, St. Louis, MO.

[20] Zheng, Q.P., Jasuja, A.K., and Lefebvre, A.H. (1996) "Influence of Air and Fuel Flows on Gas Turbine Sprays at High Pressures," *26th Symposium on Combustion*, pp. 2757-2762, The Combustion Institute, Pittsburgh, PA.

[21] Schlamp, S., Hornung, H.G., Sobota, T.H., and Cummings, E.B. (2000) "Accuracy and Uncertainty of Single-Shot Nonresonant Laser-Induced Thermal Acoustics," *Appl. Optics*, **39**, pp. 5477-5481.

[22] Danehy, P.M., Friedman-Hill, E.J., Lucht, R.P., and Farrow, R.L. (1993) "The Effects of Collisional Quenching on Degenerate Four-Wave Mixing," *Appl. Phys. B.*, Vol. 57, pp 243-248.

[23] Cummings, E. B., Leyva, I. A. and Hornung, H. G. (1995) "Laser-Induced Thermal Acoustics Signals from Finite Beams," *Appl. Opt*., **34**, pp 3290-3302.